Electronic structure of the $c(2\times2)$O/Cu(001) system

Sergey Stolbov,[1] Abdelkader Kara,[1] and Talat S. Rahman[1,2]

[1]*Department of Physics, Cardwell Hall, Kansas State University, Manhattan, Kansas 66506*

[2]*Fritz Haber Institute der Max Planck Gesselschaft, 4-6 Faraday Weg, D-14195 Berlin, FRG*

(Received 16 July 2002; published 5 December 2002)

The locally self-consistent real-space multiple-scattering technique has been applied to calculate the electronic structure and chemical binding for the $c(2\times2)$ O overlayer on Cu(001), for a set of values of $d_{\text{O-Cu1}}$, the height of O above the fourfold hollow sites, as proposed from experiment. The O-Cu bond is found to have a mixed ionic-covalent character in all cases. However, the electron charge transfer from the metal surface to O depends strongly on $d_{\text{O-Cu1}}$ and is traced to the strength of the long-range Coulomb interaction. A competition between the hybridization of Cu-d_{xz} states with O-p_x/p_y states and that of Cu-$d_{x^2-y^2}$ states with O-p_z states, is shown to control the modification of the electronic structure as O atoms approach the Cu(001) surface. Further, the O valence electronic charge density is found to be anisotropic and nonmonotonically dependent on $d_{\text{O-Cu1}}$. We compare the electronic structure of the $c(2\times2)$ O overlayer on Cu(001) and Ni(001), to draw conclusions about their relative stability.

I. INTRODUCTION

Oxygen adsorption on Cu(001) has been the subject of much discussion and debate in the past three decades mainly because of the illusive nature of the adsorption geometry. The history of the field is nicely summarized in a recent paper.[1] Here we mention some of the essential points. Unlike Ni(001) on which a true $c(2\times2)$ phase is observed[2] as the coverage approaches 0.5 ML and oxygen atoms occupy fourfold hollow sites at a distance about 0.8 Å above the top Ni layer,[3] the stable surface structure[4] for similar oxygen coverage on Cu(001) has the periodicity $(2\sqrt{2}\times\sqrt{2})R45°$ and involves missing rows of Cu atoms according to the low-energy electron-diffraction[5] (LEED) and surface x-ray-diffraction[6] measurements. This conclusion for Cu(001) was agreed upon after much debate and analysis of data from several complimentary experimental techniques, some of which indicated the presence of a $c(2\times2)$ structure on an unreconstructed Cu(001).[7–10] Other experiments have indicated the presence of both of these phases on Cu(001),[11,12] and still others have given evidence of disordered phases in the system.[13] A more recent scanning-tunneling microscopy study has also affirmed the presence of $c(2\times2)$ overlayer of adsorbed oxygen on Cu(001) at low coverage, in nanometer-size domains.[14] The picture emerging from the above findings may be summarized as follows. If the adsorbate coverage is low, oxygen atoms adsorb on Cu(001) forming $c(2\times2)$ islands. Increase in the coverage leads to the ordering of the $c(2\times2)$ domains. When the coverage approaches a critical value ($\sim34\%$ of a monolayer), the $(2\sqrt{2}\times\sqrt{2})R45°$ structure made by a missing-row-type reconstruction is formed. Nevertheless, the $c(2\times2)$ O/Cu(001) system is observed in experiments, albeit not in large domains. Structural studies of the $c(2\times2)$ O/Cu(001) system with different experimental techniques have also proposed a range (0–1.5 Å) of values for $d_{\text{O-Cu1}}$, with a majority[1,9,12] settling for 0.4 Å-0.8 Å. Furthermore, surface extended x-ray-adsorption fine-structure

measurements[12] suggest three different configurations. In one the O atoms are located at the fourfold hollow (FFH) sites with $d_{\text{O-Cu1}}=0.5$ Å, while the other two configurations represent the distorted FFH geometries with $d_{\text{O-Cu1}}=0.8$ Å. The authors of recent photoelectron-diffraction studies[1] also propose a two-site model for this system involving the O atoms at FFH positions with $d_{\text{O-Cu1}}=0.41$ and 0.7 Å, associated with the edge and center positions in small $c(2\times2)$ domains, respectively.

The competition between the observed O/Cu(001) phases and the subsequent reconstruction of the surface with the $(2\sqrt{2}\times\sqrt{2})R45°$ overlayer shows signs of a delicate balance in the surface electronic structure of the system which tilts in favor of one phase or the other depending on the coverage. There are thus two main questions for oxygen overlayers on Cu(001): what makes the $(2\sqrt{2}\times\sqrt{2})R45°$ structure stable at 0.5-ML coverage? What are the characteristics of the $c(2\times2)$ phase which appear to be present at low coverage? A related question is whether the range of values of the adsorption height reported for the $c(2\times2)$ case can be sorted through some rational criterion. Clearly, a detailed description of the electronic states and chemical bonds formed when oxygen atoms adsorb on the Cu surface would provide much needed insight into factors responsible for the observed variations in surface structure for this interesting system.

To our knowledge there is only one previous theoretical paper in which both O superstructures on Cu(001) were considered explicitly. These calculations were based on the effective medium theory[15] and predicted a reconstructed stable state for the substrate. These researchers found that the O valence levels interact very strongly with the Cu d bands such that the states can be shifted through the Fermi level. The difference in the total energy of the reconstructed and the unreconstructed Cu surfaces arises from dependence of the energetic location of the antibonding levels, derived from the $2p$O-$3d$Cu hybridization, on coordination. A missing row can force this level up, thereby pushing up the hybridized antibonding level which can straddle the Fermi level,

leading to a reduced occupation and thus stronger net bonding. A large charge transfer to the adsorbate[16,17] has also been proposed as the rationale for a reconstructed Cu surface with O as adsorbate. *Ab initio* calculations performed for oxygen on small clusters of Cu (2–25 atoms[18] and 5 atoms[17]) found a strong electronic charge transfer from the metal atoms to oxygen in the amount of $1.2e$ (Ref. 18) or $1.5e$.[17]

These two factors, the degree of the pO-dCu hybridization and amount of the effective charge on O, have thus far been proposed as the driving forces for the phase instability of the $c(2 \times 2)$ structure. It should be borne in mind, however, that models such as the effective-medium theory are at best semiempirical. Further, cluster calculations do not take into account the full lattice structure. Thus contributions such as those from the Madelung potential, which may significantly influence the subband energetic positions, the ensuing hybridization of states, and the charge distributions for the superstructures, are ignored. A comprehensive theoretical description should provide a relationship between the electronic and geometric structures of the system which includes contribution of the short- and long-range interactions.

In a recent work we have addressed the first question raised above about the rationale for the stability of the $(2\sqrt{2} \times \sqrt{2})R45°$ overlayer.[19] Our focus in the present paper is on questions about the $c(2 \times 2)$ O overlayer on Cu(001): what are the salient features of its electronic structure? How do these features depend on $d_{\text{O-Cu1}}$? For this we have carried out detailed calculations of the electronic structure of the O/Cu(001) system using a reliable method. Since the $c(2 \times 2)$O overlayer is known to be very stable on Ni(001), we have also included a selective examination of this system. Such a comparative study allows an understanding of the relative merits of the $c(2 \times 2)$O on Cu(001) and Ni(001). It also provides insights into factors controlling charge transfer and chemical bond formation in the system. It should be mentioned that electronic structure calculations of $c(2 \times 2)$ O/Ni(001) have been carried out using linear combination of atomic orbitals[20] and linear-adjugate plane-wave[21] methods. However, in both papers authors approximated the system by a slab with three Ni layers with an O overlayer. As we shall see from our calculations, such a slab is not thick enough to provide an accurate description of O/Ni(001).

If indeed an appreciable charge transfer and details of pO-dM ($M =$ Cu, Ni) hybridization are responsible for the stability of a superstructure on Cu(001), a systematic calculation of these quantities is warranted. As mentioned above, there continues to be a debate also on the height of the oxygen atoms above the Cu surface. Our calculational strategy allows us to compare the local charge redistribution, modifications of hybridization of various electronic states, and variations of the local and long-range contributions to the potentials, as a function of the height of the oxygen overlayer above the surface. It is through such systematic studies and, in conjunction with experimental observations, that we expect to gain insights into the nature of the chemical binding between the O and M atoms and establish rationale for the formation of a particular overlayer.

II. COMPUTATIONAL METHOD

The calculations are based on the density-functional theory within the local-density approximation[23] (LDA) and multiple-scattering theory. Our approach embodies the local self-consistent multiple-scattering method,[24] in which a compound is divided into overlapping clusters called local interaction zones (LIZ's) centered around atoms in different local environments. For each LIZ, a system of equations for the T-scattering matrix in the lattice site-angular momentum representation for the muffin-tin (MT) potential[25] is solved self-consistently. The solutions are used to determine the cluster Green's functions and subsequently the local and total electronic densities of states and valence charge densities. An application of this method to materials (copper oxides) related to the work here has demonstrated its high efficiency and reliability.[26,27]

In our model systems, apart from the oxygen overlayer, the top four metal layers ($M1-M4$) were taken to be different from the bulk metal. The fifth and lower metal layers were assumed to have bulk properties. LIZ's were built around nonequivalent atoms belonging to the five different layers and contained 71–79 atoms depending on the local configuration. The sizes of the LIZ's were taken such that the calculated characteristics of the bulk system closely matched those obtained from other reliable methods.

At each iteration of the self-consistent process a new potential is built by solving Poisson's equation with the charge density obtained at the previous iteration. To take into account surface effects we follow the approach developed in Ref. 28 where the MT potential at the αth atom belonging to the ith layer is given by

$$
V(r_{i\alpha}) = -\frac{2Z_{i\alpha}}{r_{i\alpha}} + 8\pi\left[\frac{1}{r_{i\alpha}}\int_0^{r_{i\alpha}} \rho_{i\alpha}(x)x^2 dx\right.
$$
$$
\left. + \int_{r_{i\alpha}}^{R_{i\alpha}} \rho_{i\alpha}(x)x dx\right] + V^{xc}[\rho(r_{i\alpha})] - V^{EC} - V^{xc}(\rho^0)
$$
$$
- 4\pi\rho_i^0 + V_{i\alpha}^{Mad}. \tag{1}
$$

The first term in Eq. (1) represents the nuclear part of the potential, where $Z_{i\alpha}$ is the nuclei charge. The terms in square brackets are the contribution of the electronic charge density $\rho_{i\alpha}(r)$ located inside the MT sphere of radius $R_{i\alpha}$, while $V^{xc}[\rho(r_{i\alpha})]$ is the exchange-correlation potential inside the MT sphere. These terms are of the same form as in the bulk calculations.[29,30] The next two terms, the electrostatic (V^{EC}) and the exchange-correlation [$V^{xc}(\rho^0)$], constitute the MT constant within which the multiple-scattering theory has to be the same for an entire system. Their values are thus taken from results of bulk calculation. The last two terms in the above expression, on the other hand, represent the distant part of the MT potential and need explicit information about the surface:

$$
V_D = -4\pi\rho_i^0 + V_{i\alpha}^{Mad}. \tag{2}
$$

For a surface system the interstitial charge density ρ_i^0 is expected to be layer dependent, reflecting the asymmetry of the

system. The space in the vicinity of the surface is divided into layers belonging to different atomic planes parallel to the surface. In the present calculations we keep the thickness of the oxygen layer independent of the O-Cu1 spacing such that the radius of the corresponding Wigner-Seitz sphere is equal to the O-*II* ionic radius $R_O = 1.24$ Å. The thickness of the Cu2 and higher layers is taken to be the bulk lattice parameter. The Cu1 layer takes the rest of the space between the O and Cu2 layers. The ρ_i^0 values are obtained by averaging the interstitial charges. The latter are differences between Wigner-Seitz ($Q_{i\alpha}^{WS}$) and MT ($q_{i\alpha}^{MT}$) charges, which are calculated by integration of the electronic charge density over Wigner-Seitz and MT spheres, respectively. The $Q_{i\alpha}^{WS}$ values are multiplied by a coefficient to meet the charge neutrality condition for the region disturbed by the surface. This coefficient approaches unity, with charge convergence. The Madelung potential itself includes the monopole $M_{i\alpha,j\beta}^{00}$, dipole $M_{i\alpha,j\beta}^{10}$, and interstitial $V_{ij}[\rho_j]$ terms:[28]

$$V_{i\alpha}^{Mad} = \sum_{j,\beta} (q_{j\beta}M_{i\alpha,j\beta}^{00} + d_{j\beta}M_{i\alpha,j\beta}^{10} + V_{ij}[\rho_j]), \qquad (3)$$

where $d_{j\beta}$ is a dipole moment of the MT charge density and

$$q_{j\beta} = Z_{j\beta} - q_{j\beta}^{MT} + \frac{4\pi}{3}\rho_j R_{j\beta}^3.$$

The $M_{i\alpha,j\beta}^{00}$ and $M_{i\alpha,j\beta}^{10}$ terms in Eq. (3) are calculated by an Ewald-like planewise summation, and explicit solution of a one-dimensional (normal to the surface) Poisson's equation, using the technique described in Ref. 28. The exchange and correlation parts of the potential are determined within LDA.[31]

To test the applicability of the method to surface problems, we have calculated the electronic structure of clean Cu(001) and found good agreement of our results with ones obtained by means of tight-binding linear muffin-tin orbital (LMTO) method,[34] a screened Korringa-Kohn-Rostoker (KKR) Green's-function method,[35] and a self-consistent localized KKR scheme developed for the surface calculations.[28] Our projected densities of electronic states calculated for the $c(2 \times 2)$ O/Cu(001) system are also found to be in good agreement with those obtained by the full potential LMTO method.[22]

III. RESULTS AND DISCUSSION

We present here results for the calculated electronic structure of the $c(2 \times 2)$O overlayer on Cu(001) for selected values of $d_{\text{O-Cu1}}$, with O occupying the fourfold hollow site. Keeping in mind the discrepancy in the values of $d_{\text{O-Cu1}}$ obtained from different experiments, we have varied it between 0.54 Å and 1.08 Å in our calculations and examined its effect on the surface electronic structure. Included also are the results of a similar O overlayer on Ni(001), for which we have performed calculations with $d_{\text{O-Ni1}} = 0.7$ Å, and 0.81 Å. Note that the latest LEED data give an experimental value of 0.72 Å (Ref. 32) for $d_{\text{O-Ni1}}$, while previously 0.77 Å,[3] and originally 0.9 Å (Ref. 33) had been proposed. Our point is to
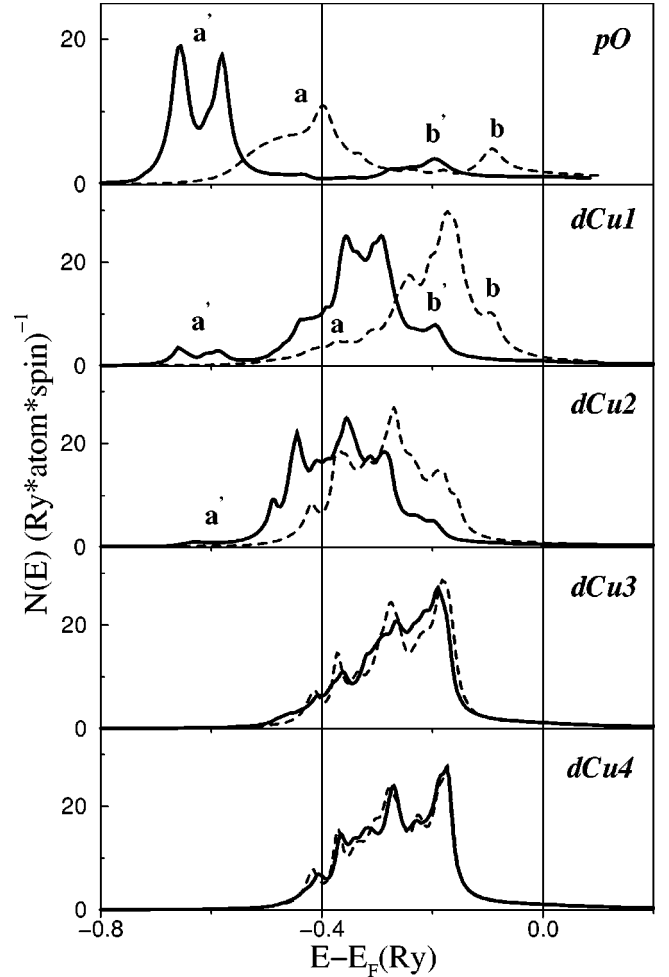

FIG. 1. The density of *p*-electronic states of the oxygen overlayer and *d*-electronic states of the four top Cu layers for O/Cu(001) for O-Cu1 interlayer spacings of 1.08 Å (dashed line) and 0.54 Å (solid line).

examine the effect of slight variation of the height, at which the adsorbate sits, on the electronic structure of the two systems. In each case under consideration, the local densities $N_l^\alpha(E)$ of electronic states, their projection $N_{lm}^\alpha(E)$ on the cubic harmonics, and the valence electron density $\rho(r)$ have been calculated for the oxygen overlayer and the four top metal layers.

For the longest and shortest $d_{\text{O-Cu1}}$ considered, the densities of the *p*O and *d*Cu electronic states of the system are plotted in Fig. 1. Clearly, the $N_d^{Cu}(E)$ for Cu3 and Cu4 (i.e., atoms in the third and fourth layers) are hardly affected by the choice of $d_{\text{O-Cu1}}$ and they resemble each other (they are almost bulklike), while those for Cu2 show a dependence on the height at which O sits. The *d*Cu2 states appear also to be distinct from the ones in the layers below. Furthermore, the *d*Cu1 and *p*O densities exhibit a rich structure and for both values of $d_{\text{O-Cu1}}$ the spectra show a clear signature of the *p*O-*d*Cu1 hybridization. Note the position of the peaks marked "*a*" and "*b*" for $d_{\text{O-Cu1}} = 1.08$ Å and "*a'*" and "*b'*" for $d_{\text{O-Cu1}} = 0.54$ Å in Fig. 1. As the oxygen overlayer gets closer to the Cu(001) surface, the splitting (the distance
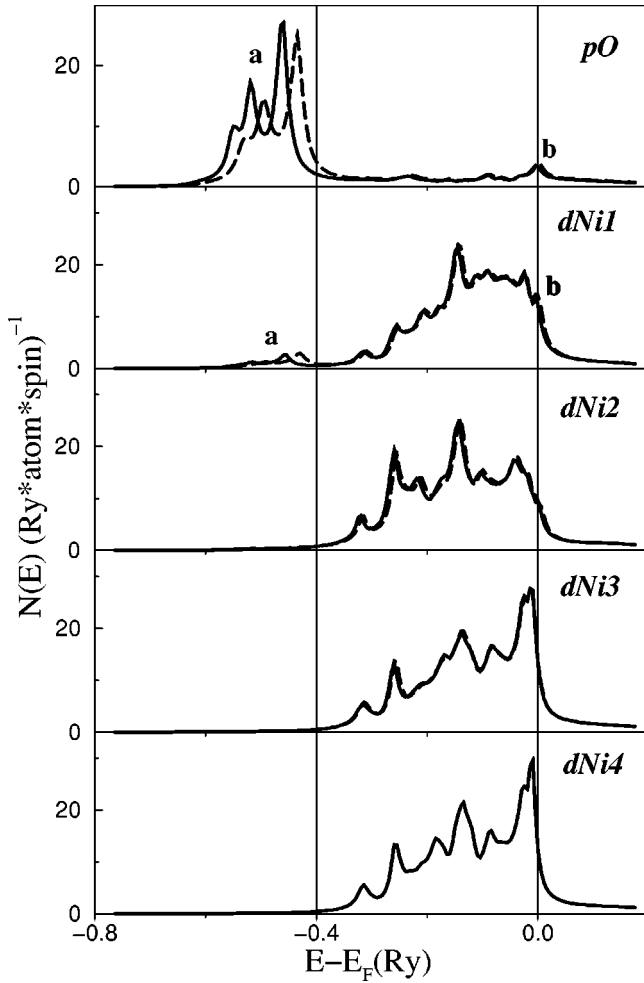
FIG. 2. The density of p-electronic states of the oxygen over-layer and d-electronic states of the four top Ni layers for O/Ni(001) for O-Ni1 interlayer spacings of 0.81 Å (dashed line) and 0.7 Å (solid line).

FIG. 3. Upper panel: the layer charges per 2D unit cell calculated for O/Cu(001) with $d_{O\text{-}Cu1} = 1.08$ Å (open circles) and 0.54 Å (filled circles), and O/Ni(001) with $d_{O\text{-}Ni1} = 0.7$ Å (triangles). The layer numbered 0 corresponds to the oxygen overlayer. Lower panel: charge deviation for the oxygen overlayer on Cu(001) (filled circles), on Ni(001) (open circles), and the distant part of the MT potential at the O sites for O/Cu(001) (filled triangles) and for O/Ni(001) (open triangles) plotted versus the adsorbate height.

between a-b or a'-b' peaks in the figure) increases, reflecting an enhancement of covalent bonding.

The densities of the pO and dNi states calculated for the $c(2\times2)$ oxygen overlayer on Ni(001) with two values $d_{O\text{-}Ni1}$ are shown in Fig. 2. The covalent contribution to the bonding is again signified by the splitting between the pO and dNi1 states (peaks "a" and "b") in the figure. Note that in the case of O/Ni(001) the antibonding pO peak "b" is located at the Fermi level, in agreement with the x-ray and photoelectron spectroscopic measurements.[36] Figure 2 also shows that unlike the case of O/Cu(001) in which the local densities of state of the two top Cu layers were significantly perturbed by the presence of the overlayer, the Ni-d subband of the top four layers are aligned with each other. This difference may be attributed to the high density of Ni-d states at the Fermi level E_F. Under such conditions even a small shift of a subband, resulting from a local potential perturbation, produces a change in the local charge, large enough to screen the perturbation. Therefore such subbands are "pinned" to the Fermi level. Another difference from Figs. 1 and 2 is that the p-d splitting is higher in O/Ni(001) than in O/Cu(001),

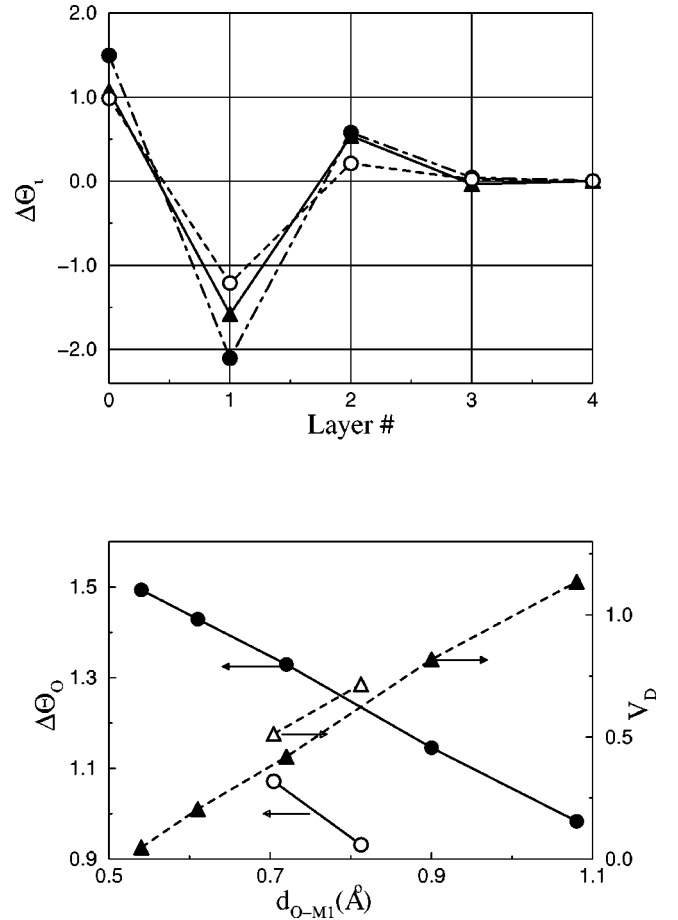for the chosen values of d_{O-M1}, where $M1$ may be Ni1 or Cu1. Covalent bonding is thus found to be stronger in the case of the former than in the latter.

To examine charge transfer in the vicinity of the surface, we have calculated Wigner-Seitz charges from which we have determined the charge deviation (ΔQ_i) from electric neutrality, per two-dimensional(2D) unit cells belonging to the different layers. The results for $d_{O\text{-}Cu1} = 1.08$ Å and 0.54 Å are shown in the upper panel of Fig. 3. One can see a strong charge transfer from the top metal layer to the O overlayer, coupled with some increase in the electron charge in the second metal layer. The effect is significantly enhanced when the oxygen atoms approach the Cu1 layer. In Table I, we present the amount of charge transfer for five different heights of the oxygen overlayer that we considered for the O/Cu(001) system. At the shortest O-Cu1 distance, the two Cu atoms in the unit cell of the first layer have a deficit of about one electron each, with $1.5e$ going to the O atom and $0.25e$ for each of the two atoms of the second layer. The amount of charge provided to the O atom drops to $1e$ when

TABLE I. Valence electronic charge variation $\Delta Q(e)$ for several O-Cu1 spacings for O/Cu(001). The percentages in parentheses are a change of the Wigner-Seitz charge with respect to the bulk for Cu and to the atomiclike for O.

Layer	0.54 Å	0.61 Å	0.72 Å	0.9 Å	1.08 Å
O	1.493 (37.3%)	1.429 (35.7%)	1.329 (33.2%)	1.144 (28.6%)	0.983 (24.6%)
Cu1	−2.108 (−9.6%)	−1.986 (−9.0%)	−1.800 (−8.2%)	−1.484 (−6.8%)	−1.211 (−5.5%)
Cu2	0.575 (2.6%)	0.519 (2.4%)	0.430 (2.0%)	0.313 (1.4%)	0.207 (0.9%)
Cu3	0.040 (0.2%)	0.039 (0.2%)	0.041 (0.2%)	0.027 (0.1%)	0.021 (0.1%)
Cu4	0.000 (0.0%)	0.000 (0.0%)	0.000 (0.0%)	0.000 (0.0%)	0.000 (0.0%)

its height above Cu1 is doubled to 1.08 Å. It should be pointed that the layer charge deviation on clean Cu(001) (Ref. 19) is found to be less than $0.1e$ ($0.05e$ per Cu atom). From these results one would conclude that the O-Cu1 chemical binding has an essentially ionic character and that the ionicity increases as oxygen atoms approach the metal surface. In Fig. 3, we also find an appreciable charge transfer to the O layer in the O/Ni(001) case and the trends are similar, but quantitatively different, from those for O/Cu(001). The layer-by-layer, variations of charge transfer, for two plausible values of $d_{\text{O-Ni1}}$, are summarized in Table II. Their comparison with the respective values in Table I shows subtle differences between the two systems.

The dependence on $d_{\text{O-M1}}$ of the charge deviation ΔQ_O of the O layer, and that of the distant part V_D of the potential in Eq. (2) at the O site, are plotted in the lower panel of Fig. 3. A clear correlation between ΔQ_O and V_D seen in the figure suggests that the long-range electrostatic interaction is a driving force for the charge transfer in both systems.

In the systems under consideration, each oxygen atom and its four-nearest metal neighbors form a pyramid. Such an atomic configuration is expected to cause a strong anisotropy in the electronic structure. Therefore an analysis of the $N_{lm}^{\alpha}(E)$ projections for O and $M1$ is very useful for understanding the nature of the chemical bonds formed when oxygen adsorbs on the metal surfaces. A simple symmetry consideration (see Fig. 4) shows that only the O-p_x, p_y-$M1$-d_{xz}, and O-p_z-$M1$-$d_{x^2-y^2}$ hybridization can be significant in the O-$M1$ subsystem. Therefore our focus is mainly on these electronic states. In Fig. 5, the densities of the O-p_z and Cu1-$d_{x^2-y^2}$ states are plotted, for the values of $d_{\text{O-Cu1}}$ as labeled. Both projected densities are considerably modified with the decrease in $d_{\text{O-Cu1}}$. The band broadens and distinct new peaks appear as $d_{\text{O-Cu1}}$ takes the values 0.72 Å and 0.54 Å. An energetic alignment of the O-p_z and Cu1-$d_{x^2-y^2}$ peaks

in the a, b, and c regions is a signature of hybridization of these states. An increase in the peak amplitudes and an extra splitting with the decrease in $d_{\text{O-Cu1}}$ reflect a strong enhancement of the hybridization as the oxygen atoms approach the surface. In contrast, the splitting of the O-p_x, p_y and Cu1-d_{xz} states is almost independent of the $d_{\text{O-Cu1}}$ value (see Fig. 6). This means that the hybridization of these states is not changed noticeably, as $d_{\text{O-Cu1}}$ is varied within the range considered. Such a difference in the response of the electronic states to variation of $d_{\text{O-Cu1}}$ can be explained on the basis of a simple geometric analysis. When oxygen atoms approach the Cu1 layer, the O-Cu1 bond length decreases and the symmetry of the O-p_z and Cu1-$d_{x^2-y^2}$ cubic harmonics is such that their overlap increases (see Fig. 4) enhancing the hybridization. On the other hand, the symmetry of the O-p_x, p_y and Cu1-d_{xz} states is such that the overlap of their cubic harmonics is diminished with a decrease in $d_{\text{O-Cu1}}$ that compensates the effect of the O-Cu1 bond-length reduction. Thus, a noticeable covalent pO-dCu1 contribution to binding takes place, along with the strong ionic binding discussed above. If the O-Cu1 spacing is long enough
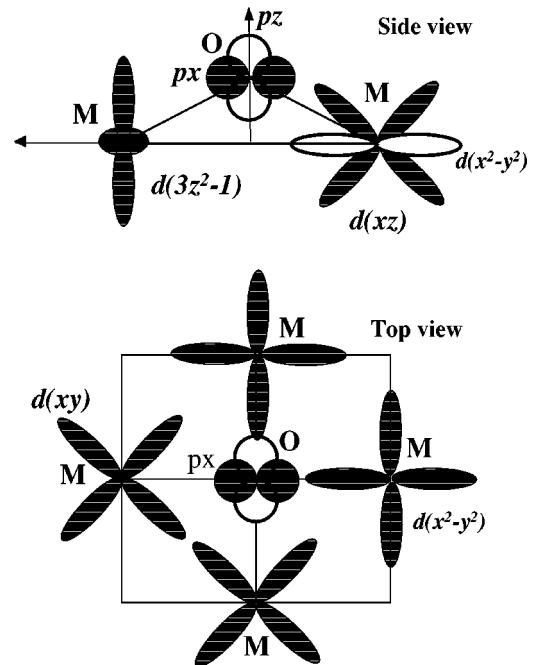
TABLE II. Same as in Table I but for O/Ni(001).

Layer	0.7 Å	0.81 Å
O	1.071(26.8%)	0.931(23.3%)
Ni1	−1.585(−7.9%)	−1.333(−6.7%)
Ni2	0.535(2.7%)	0.409(2.0%)
Ni3	−0.04(−0.2%)	−0.027(−0.1%)
Ni4	0.019(0.1%)	0.02(0.1%)
Ni5	0.0(0.0%)	0.0(0.0%)

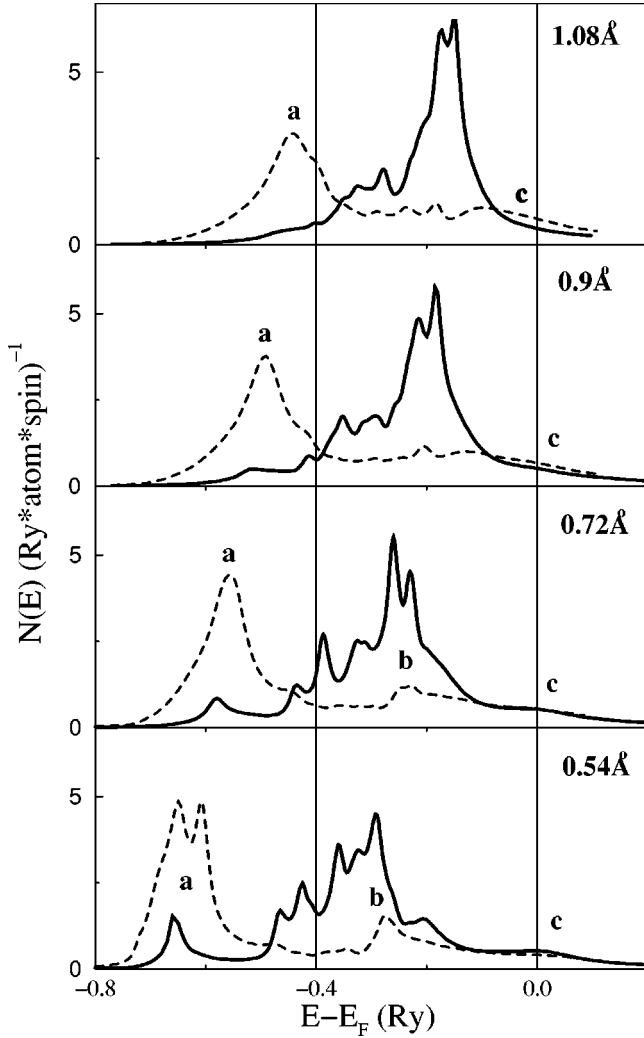FIG. 4. Schematic illustration of the pO- and dM1-cubic harmonics in the $c(2\times2)$O/M(001) system.

FIG. 5. The densities of the O-p_z (dashed line) and Cu1-$d_{x^2-y^2}$ (solid line) electronic states for $c(2\times2)$O/Cu(001) with different O-Cu1 interlayer spacings.

FIG. 6. The densities of the O-$p_{x,y}$ (dashed line) and Cu1-d_{xz} (solid line) electronic states for $c(2\times2)$O/Cu(001) with different O-Cu1 interlayer spacings.

($d_{\text{O-Cu1}} = 1.08$ Å), the covalent component of chemical binding is mostly determined by the O-p_x, p_y-Cu1-d_{xz} hybridization. On the other hand, for smaller values of $d_{\text{O-Cu1}}$, the O-p_z-Cu1-$d_{x^2-y^2}$ contribution is more prominent. The competition between these two factors controls the modifications of the electronic states as oxygen atoms approach the surface.

The densities of O-p_x, -p_y, and O-p_z electronic states have also been calculated for the O/Cu(001) by means of the full potential LMTO method,[22] which is considered to be one of the most reliable approaches for electronic structure calculations. These authors considered an oxygen overlayer with a $c(2\times2)$ structure with the oxygen atom occupying both FFH and quasi-FFH sites. A comparison of our results with those from Ref. 22 shows that both the splitting and relative peak amplitudes are in very good agreement, thereby attesting to the reliability of the method used here.

Before closing the discussion on $N_{lm}^{\alpha}(E)$ which we find to have similar trends on O/Cu(001) and O/Ni(001), we turn to a quantitative measure of the magnitude of covalent splitting
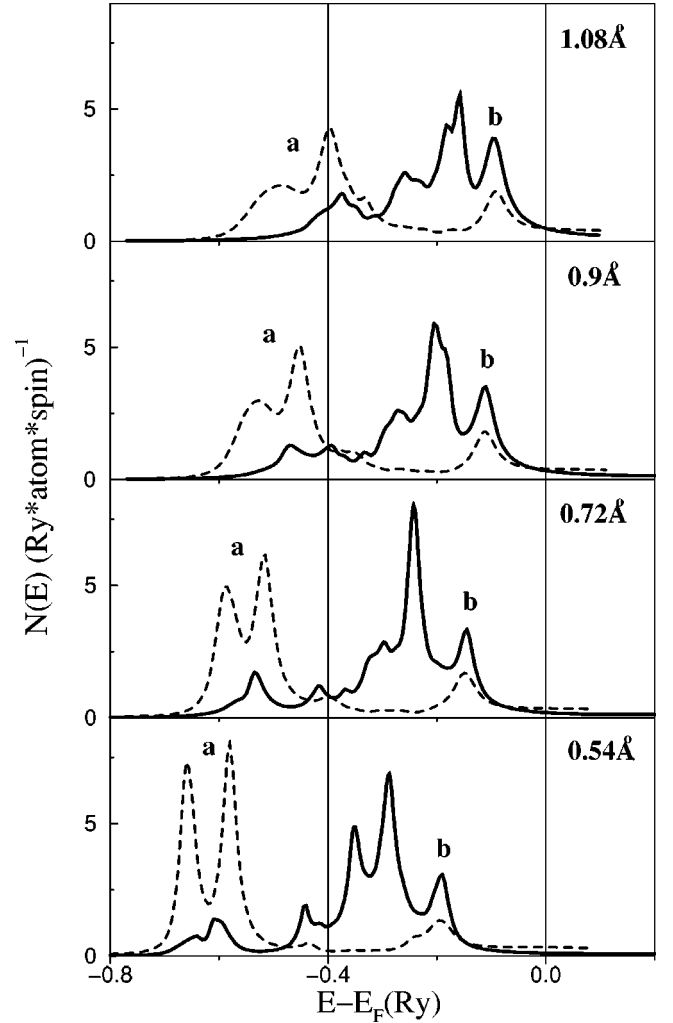
in the two systems in Fig. 7. We find the energetic separation between the higher peak in the bonding O-$p_{x,y}$ peak [peak a for O/Ni(001) and peak a' for O/Cu(001)], and the antibonding peak [b for O/Ni(001) and b' for O/Cu(001)], to be 0.37 Ry and 0.46 Ry, for O/Cu(001) and O/Ni(001), respectively. Thus, for almost the same value of $d_{\text{O-M1}}$ [0.72 Å for O/Cu(001) and 0.7 Å for O/Ni(001)] the splitting is found to be 24% higher for O/Ni(001) than for O/Cu(001). Although for the O-p_z subband it is harder to quantify the splitting, Fig. 7 indicates that these subbands are also split more strongly for O/Ni(001) than for O/Cu(001). This finding can be explained with ease if we compare the degree of localization of the dCu and dNi wave functions. The latter, being more extended, provides higher spatial overlap and stronger covalent bonding for the pO-dNi states, as compared to the situation for pO-dCu.

Finally, we turn to the calculated radial dependence of the valence electron charge density around the O and Cu1 – Cu4 atoms along some high-symmetry directions. The results indicates that the oxygen charge density is essentially anisotropic. We also find that the anisotropy increases when
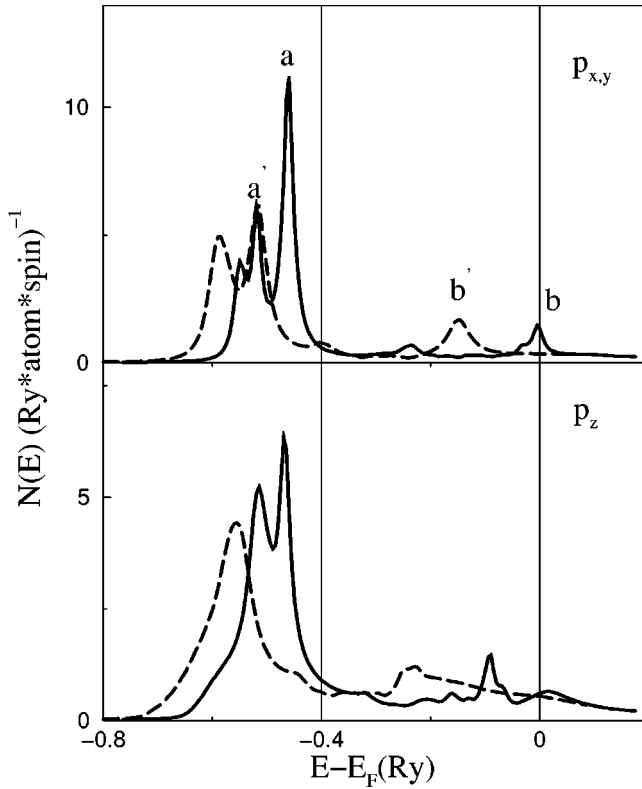
FIG. 7. The densities of the O-$p_{x,y}$ (upper panel) and O-p_z (lower panel) electronic states calculated for O/Cu(001) (dashed line) and for O/Ni(001) (solid line).

$d_{\text{O-Cu1}}$ is reduced from 1.08 Å to 0.72 Å, whereas further $d_{\text{O-Cu1}}$ reduction leads to a decrease in the anisotropy. This effect is illustrated in Fig. 8, in which the radial dependence of the difference in the densities along the (001) and (100) directions is plotted for three values of $d_{\text{O-Cu1}}$. Such a non-monotonic behavior can be explained by the hybridization competition mentioned above. The reversal in the anisotropy of the oxygen charge density in Fig. 8 is ultimately related to
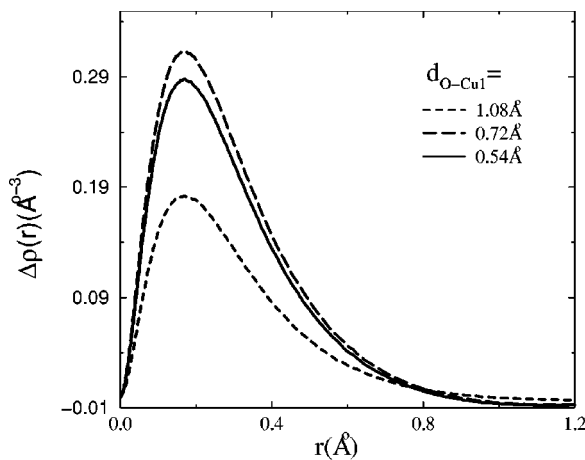

FIG. 8. The radial dependence of the difference between the oxygen valence electron charge densities calculated along the (001) and (100) directions for O/Cu(001) with three different O-Cu1 interlayer spacings.

the relative amounts of charge flow to the O-p_x and O-p_z states, for a specific $d_{\text{O-Cu1}}$. The stronger the covalent binding, the larger is the increase in the electron-electron repulsion caused by an extra electronic charge in the bond region. Therefore the charge tends to go to the states less involved in hybridization, which are the O-p_z states for larger values of $d_{\text{O-Cu1}}$. This leads to an increase in the anisotropy. The tendency is reversed at short O-Cu1 distances, in which the hybridization of the O-p_z and Cu1-$d_{x^2-y^2}$ is enhanced significantly, making the charge transfer to the O-p_x, -p_y states more preferable.

The results presented above provide the following microscopic picture for the interaction between the $c(2\times2)$O overlayer and Cu(001) and Ni(001). A reduction of the oxygen-metal spacing leads to two effects: (i) an increase in the long-range Coulomb interaction which pushes down the local potentials at the O sites and through it induces electronic charge transfer from the host surface to the O atoms; and (ii) an enhancement of the covalent pO-dM1 binding. The first effect is expected to increase the total energy of the system because of enhancement of the electron-electron repulsion caused by the increase in the electronic density at the O atoms. The second effect, on the other hand, reduces the total energy. Relative magnitudes of these two effects are different for O/Cu(001) and O/Ni(001). Since the dNi wave function is more extended than the dCu wave function, the covalent pO-dM1 binding for equivalent O-M1 spacing is stronger in O/Ni(001) than in O/Cu(001). In addition, the charge transfer is smaller in O/Ni(001) than in O/Cu(001). It is thus plausible that in O/Ni(001) the competition of the two effects leads to a minimum in total energy at certain values of $d_{\text{O-Ni1}}$ making the $c(2\times2)$ structure stable, whereas in O/Cu(001) such a minimum does not occur because of a relative weakness of the covalent bonds and strength of the Coulomb repulsion.

We now turn to the application of the results presented here to a simple model for oxygen adsorption on Cu(001) proposed by Lederer et al.,[12] centered around an isotropic model potential based on the local part of the Madelung potential. We agree with the authors that not only are the O and Cu1 layers involved in charge transfer, but also deeper ones, and that the charges and covalence of the bonds are smooth functions of the interatomic distance. However, the essential difference between the $c(2\times2)$ and $(2\sqrt{2}\times\sqrt{2})R45°$ phases lies in the differences in the symmetry of the oxygen local surrounding rather than in $d_{\text{O-Cu1}}$. This suggests that the phase transition can be properly described only by means of an anisotropic potential. Moreover, a noticeable covalence of the O-Cu1 binding (even for relatively long bond lengths) and its anisotropy obtained in our study indicates that an accurate modeling of the $c(2\times2)$ phase itself requires an anisotropic potential.

IV. CONCLUSIONS

The electronic structure has been calculated for the $c(2\times2)$ O/Cu(001) and O/Ni(001) systems for several O-M1 interlayer spacings. We find that the oxygen and metal atoms form a mixed ionic-covalent chemical bond in the O/M(001)

system for all plausible values of the O-$M1$ interlayer spacings. Reduction of the O-$M1$ spacing causes an enhancement of the pO-$dM1$ covalent binding and an increase in the long-range Coulomb interaction followed by charge transfer from the metal surface to oxygen. We find that a competition between these two factors determines features of the energetic profiles of the systems. Because the dNi wave function is more extended than the dCu wave function, the covalent binding is stronger in O/Ni(001) than in O/Cu(001). Furthermore, the charge transfer in the former is lower than in the latter. These factors provide a rationale for the stability of the $c(2\times2)$ phase on O/Ni(001), as compared to that on O/Cu(001). Detailed analysis of the properties of the local electronic structure reveals that the electronic structure of the O/Cu(001) system is governed by a competition between the hybridization of Cu1-d_{xz}-O-p_x, p_y and Cu1-$d_{x^2-y^2}$-O-p_z states, which depends on O-Cu1 spacing. The anisotropy of the oxygen valence electron charge density is found to be strongly and nonmonotonically dependent on the interlayer spacing.

[1] M. Kittel, M. Polcik, R. Terborg, J.-T. Hoeft, P. Baumgärtel, A.M. Bradshaw, R.L. Toomes, J.-H. Kang, D.P. Woodruff, M. Pascal, C.L.A. Lamont, and E. Rotenberg, Surf. Sci. **470**, 311 (2001).

[2] J.E. Demuth, D.W. Jepsen, P.M. Marcus, Phys. Rev. Lett. **31**, 540 (1970).

[3] W. Oed, H. Lindner, U. Starke, K. Heinz, K. Müller, Surf. Sci. **224**, 179 (1989).

[4] M. Wuttig, R. Franchy, and H. Ibach, Surf. Sci. **213**, 103 (1989).

[5] A. Atrie, U. Bardi, G. Casalone, G. Rovida, and E. Zanazzi, Vacuum **41**, 333 (1990).

[6] I.K. Robinson, E. Vlieg, and S. Ferrer, Phys. Rev. B **42**, 6954 (1990).

[7] S. Kono, S.M. Goldberg, N.F.T. Hall, and C.S. Fadley, Phys. Rev. Lett. **41**, 1831 (1978).

[8] S.P. Holland, B.J. Garrison, and N. Winograd, Phys. Rev. Lett. **43**, 220 (1979).

[9] U. Döbler, K. Baberschke, J. Stöhr, and D.A. Outka, Phys. Rev. B **31**, 2532 (1985).

[10] M. Sotto, Surf. Sci. **260**, 235 (1992).

[11] J.G. Tobin, L.E. Klebanoff, D.H. Rosenblatt, R.F. Davis, E. Umbach, A.G. Baca, D.A. Shirley, Y. Huang, W.M. Kang, and S.Y. Tong, Phys. Rev. B **26**, 7076 (1982).

[12] T. Lederer, D. Arvanitis, G. Comelli, L. Tröger, and K. Baberschke, Phys. Rev. B **48**, 15 390 (1993).

[13] F.M. Leibsle, Surf. Sci. **337**, 51 (1995).

[14] T. Fujita, Y. Okawa, Y. Matsumoto, and K.I. Tanaka, Phys. Rev. B **54**, 2167 (1996).

[15] K.W. Jacobsen and J.K. Norskov, Phys. Rev. Lett. **65**, 1788 (1990).

[16] E.A. Colbourn and J.E. Inglesfield, Phys. Rev. Lett. **66**, 2006 (1991).

[17] P.S. Bagus and F. Illas Phys. Rev. B **42**, 10 852 (1990).

[18] P.V. Madhavan and M.D. Newton, Chem. Phys. **86**, 4030 (1987).

[19] S. Stolbov and T. S. Rahman, J. Chem. Phys. **117**, 8523 (2002).

[20] C.S. Wang and A.J. Freeman, Phys. Rev. B **19**, 4930 (1979).

[21] R.W. Godby, G.A. Benish, R. Haydock, and V. Heine, Phys. Rev. B **32**, 655 (1985).

[22] T. Wiell, J.E. Klepeis, P. Bennich, O. Björneholm, N. Wassdahl, and A. Nilsson, Phys. Rev. B **58**, 1655 (1998).

[23] W. Kohn and L.J. Sham, Phys. Rev. **140**, A1133 (1965).

[24] Y. Wang, G.M. Stocks, W.A. Shelton, D.M.C. Nicholson, Z. Szotek, and W.M. Temmerman, Phys. Rev. Lett. **75**, 2867 (1995).

[25] J.S. Faulkner and G.M. Stocks, Phys. Rev. B **21**, 3222 (1980).

[26] S.V. Stolbov, J. Phys.: Condens. Matter **9**, 4691 (1997)

[27] S. Stolbov, M. Mironova, and K. Salama, Supercond. Sci. Technol. **12**, 1071 (1999).

[28] L. Szunyogh, B. Ujfalussy, P. Weinberger, and J. Kollar, Phys. Rev. B **49**, 2721 (1994).

[29] J.F. Janak, Phys. Rev. B **9**, 3985 (1974).

[30] P.C. Schmidt, Phys. Rev. B **31**, 5015 (1985).

[31] O. Gunnarsson and B.I. Lundqvist, Phys. Rev. B **13**, 4274 (1976).

[32] K. Heinz, W. Oed, and J.B. Pendry, Phys. Rev. B **41**, 10 179 (1990).

[33] J.E. Demuth, D.W. Jepsen, and P.M. Marcus, Phys. Rev. Lett. **31**, 540 (1973).

[34] J. Kudrnovsky, I. Turek, V. Drchal, P. Weinberger, S.K. Bose, and A. Pasturel, Phys. Rev. B **47**, 16 525 (1993).

[35] K. Wildberger, R. Zeller, and P.H. Dederichs, Phys. Rev. B **55**, 10 074 (1997).

[36] H. Tillborg, A. Nilsson, T. Wiell, N. Wassdahl, N. Må rtensson, and J. Nordgern, Phys. Rev. B **47**, 16 464 (1993).